Multiparametric Magneto-fluorescent Nanosensors for the Ultrasensitive Detection of *Escherichia coli* O157:H7

Tuhina Banerjee,* Shoukath Sulthana,|| Tyler Shelby,|| Blaze Heckert, Jessica Jewell, Kalee Woody, Vida Karimnia, James McAfee, and Santimukul Santra*

Department of Chemistry, Kansas Polymer Research Center, Pittsburg State University, 1701 South Broadway Street, Pittsburg, Kansas 66762, United States

Ⓢ *Supporting Information*

ABSTRACT: Enterohemorrhagic *Escherichia coli* O157:H7 presents a serious threat to human health and sanitation and is a leading cause in many food- and waterborne ailments. While conventional bacterial detection methods such as PCR, fluorescent immunoassays and ELISA exhibit high sensitivity and specificity, they are relatively laborious and require sophisticated instruments. In addition, these methods often demand extensive sample preparation and have lengthy readout times. We propose a simpler and more sensitive diagnostic technique featuring multiparametric magneto-fluorescent nanosensors (MFnS). Through a combination of magnetic relaxation and fluorescence measurements, our nanosensors are able to detect bacterial contamination with concentrations as little as 1 colony-forming unit (CFU). The magnetic relaxation property of our MFnS allow for sensitive screening at low target CFU, which is complemented by fluorescence measurements of higher CFU samples. Together, these qualities allow for the detection and quantification of broad-spectrum contaminations in samples ranging from aquatic reservoirs to commercially produced food.

KEYWORDS: *E. coli* O157:H7, magneto-fluorescent nanosensor, magnetic relaxation, fluorescence emission, rapid detection of pathogen, bacterial contamination
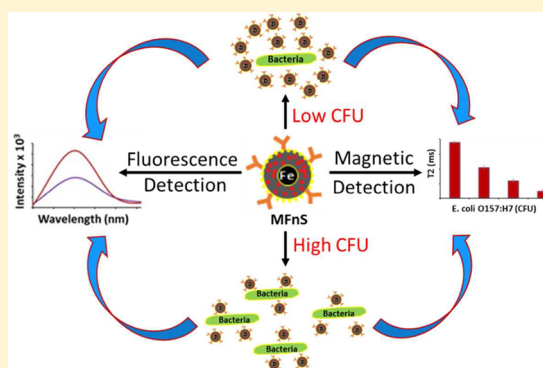
Bacterial contamination is one of the leading causes of both waterborne and foodborne illnesses and deaths and has been increasing in severity.[1,2] Many environmental water sources are contaminated with pathogenic bacterial species, including those within the *Vibrio, Salmonella, Shigella, Staphylococcus, Listeria, Campylobacter, Bacillus,* and *Escherichia* genera.[3,4] These bacterial pathogens are known to result in cholera, gastroenteritis, typhoid fever, and a number of diarrheal responses.[3] In addition, food contamination has led to outbreaks of illnesses that require massive recall efforts on behalf of the food distributors in attempts to curb the outbreak.[5−7] It has been estimated that pathogens cause 9.4 million cases of foodborne illness in the United States each year and that almost half of those cases are due to bacterial contamination.[8] Enterohemorrhagic *Escherichia coli* O157:H7 is of special note, as it has been strongly associated with both food and water contamination, antagonizing many efforts to make clean water and safe food a commodity worldwide.[1,5,9]

This pathogenic strain of *E. coli* has been observed to cause acute diarrhea and gastroenteritis when consumed via contaminated drinking water and is responsible for a number of recent foodborne illness outbreaks.[5] This serotype of *E. coli* also produces Shiga-like toxins, and infection has been observed to result in acute renal failure in a number of cases.[10] In cases where cattle, one of the primary reservoirs, come into contact

with ponds, lakes, or streams, there is a risk of contamination via fecal matter.[10] Although this does not pose a risk in areas where all drinking water is sanitized, it remains an issue for developing countries. Additionally, this serotype of *E. coli* is associated with outbreaks stemming from consumption of fruits or vegetables that have come in contact with fecal matter at some point during their processing or handling.

To prevent such detrimental infections from occurring, there have been many efforts to design techniques by which water sources or food may be scanned for pathogenic bacteria before consumption or vending. Efficient diagnostic techniques must be able to quickly detect the presence of *E. coli* O157:H7 in trace quantities, as the required cell count for infection is relatively low.[11,12] The simplest and most conventional bacterial detection technique is the culturing of microorganism samples on agar. Identification of the bacteria is accomplished via a series of biochemical tests. Although these tests are generally inexpensive and simple, they are extremely inefficient with regard to time. To produce a more time-efficient diagnostic technique, a number of methods have been developed for pathogen detection, including nucleic acid amplification (PCR variations) and detection,[2,13−15]

Scheme 1. Schematic Representation of MFnS Synthesis and the Mechanism of Dual-Mode Detection of Bacterial Contamination[a]
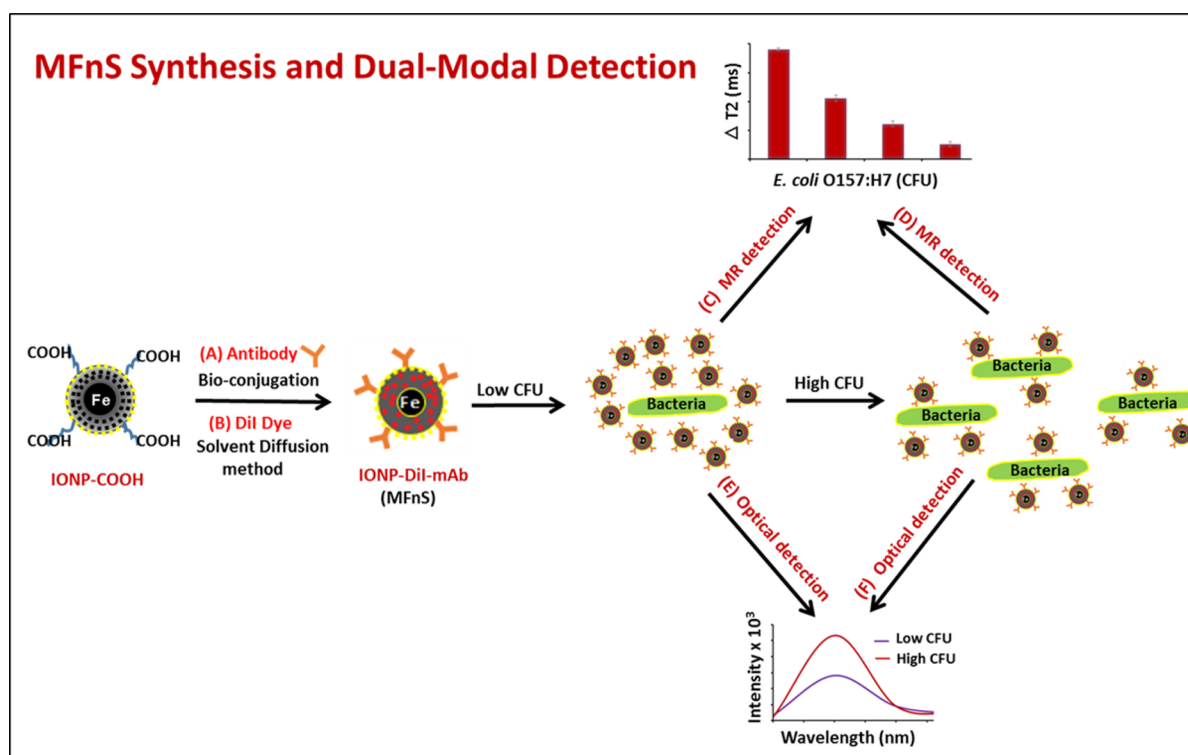
[a]Upon incubation (∼30 min), new MFnS are able to sensitively detect the target bacteria (low to high CFU) via both magnetic resonance and fluorescence intensity.

ELISA,[2,16,17] LAMP,[18] immunomagnetic and electrochemical detection via magnetic beads,[2,19] monitoring the rate of β-D-glucuronidase activity,[20] and nanoparticle-mediated fluorescence identification via targeted nanomaterials.[2,10,21−24] These methods are leaps and bounds ahead of bacterial culturing with regard to time, and each possesses its own particular benefits, but they still face a number of hurdles including false positives/negatives, cost, and complexity.[2,4] Furthermore, the majority of the current diagnostic techniques rely heavily on sample amplification and often require enrichment steps for accurate detection readings.[11] A few diagnostic techniques that do not require extensive amounts of sample amplification are detection via magnetic resonance and fluorescence.[10,25,26] In general, these modalities allow for quick sample preparation and have low turnaround times. However, in the realm of bacterial detection, each technique still has its own limitations. Magnetic nanoparticles allow for extremely sensitive and rapid detection of low colony-forming unit (CFU) bacterial contaminations, but become less quantitatively accurate as the concentration of bacteria increases. On the other hand, fluorescence detection is less sensitive with samples of dilute bacteria, but will provide strong intensity readings for higher concentrations of bacterial contamination. Herein, we propose for the first time the development of multimodal magneto-fluorescent nanosensors (MFnS) that combine these two modalities (magnetic and optical), overcoming the previous limitations. Our MFnS design provides a robust diagnostic tool capable of collecting point-of-care data, useful for detecting and monitoring bacterial contaminations in both early- and late-stage development. Furthermore, our MFnS have been tested in a variety of media and have shown that the pairing of these modalities allows for

specific detection of *E. coli* O157:H7 regardless of the source of contamination.

RESULTS AND DISCUSSION

Taking into account the limitations faced by magnetic relaxation and fluorescence independently, we have designed dual-functionalized nanosensors that combine both detection modalities in an effort to overcome their respective hurdles. Toward this end, the poly(acrylic acid) (PAA)-coated iron oxide nanoparticles (IONPs) were synthesized using our previously reported method[27,28] (Supporting Information, Scheme S1), and a monoclonal IgG1 antibody (Ab) specific for *E. coli* O157:H7 was conjugated to it using water-based carbodiimide chemistry.[27] Briefly, IgG1 Ab (10 mmol) was conjugated with surface carboxylic acid groups of IONPs ([Fe] = 5 mmol) in the presence of 1-ethyl-3-(3-(dimethylamino)-propylcarbodiimide hydrochloride (EDC; 10 mmol) and *N*-hydroxysuccinimide (NHS; 10 mmol), and the reaction was carried out at room temperature for 3 h and continued at 4 °C overnight (Scheme 1A). The resulting Ab-conjugated IONPs were purified using a magnetic column and stored in PBS (1×, pH 7.4) at 4 °C. Binding between our nanosensors and the targeted bacteria is made visible first by the collection of magnetic relaxation data, represented in Scheme 1C,D. We hypothesized that when our nanosensors are placed in solution with bacterial colonies, they will swarm around the bacteria's outer membrane due to the specific interactions between the IgG1 Ab and bacterial epitope. As a result of this clustering, the interaction between the magnetic nanosensors and their aqueous environment (water protons) is inhibited; thus, the corresponding magnetic relaxation time ($T2$ ms) increases. In

the presence of a low CFU, there is a large degree of magnetic nanosensor clustering, resulting in a larger $\Delta T2$ value. However, if the CFU count is raised, the nanosensors disperse throughout the given voxel along with the additional bacteria. As a result, the clustering is reduced, leading to smaller $\Delta T2$ values, indicating that detection via magnetic relaxation is highly sensitive for early-stage bacterial contamination. Although $\Delta T2$ values are reported for higher CFU ranges, they are less quantitatively accurate and are unable to discriminate between two high CFU solutions. Due to this, it is necessary to pair this MR modality with fluorescence detection, which is highly accurate in high CFU ranges. Together, this dual-modal detection technique would be highly accurate in both low and high CFU solutions.

To incorporate the fluorescence modality, the lipophilic optical dye, DiI (2 μL, 2 mmol), is encapsulated within the PAA coatings of IgG1-conjugated IONPs (4 mL, [Fe] = 3.5 mmol), using a previously reported solvent diffusion method (Scheme 1B).[27] The resulting MFnS are purified using a magnetic column and also by dialysis (MWCO = 6000−8000) against PBS solution (1×, pH 7.4) and found to be stable for long periods of time (Supporting Information, Table S1). The purified MFnS ([Fe] = 2 mmol) may then be incubated with bacterial solutions for the sensitive detection of high CFU samples (Scheme 1E,F). Centrifugation of these solutions will cause the bacteria and any bound MFnS to separate from any nonbound MFnS in the supernatant. The collected bacterial pellets may then be resuspended and analyzed via fluorescence. We hypothesize that in the case of a low CFU count, only a small number of nanosensors will be present in the resuspension, leading to a low fluorescence emission value. Alternatively, a high CFU count will lead to a more prominent presence of nanosensors in the resuspension and a corresponding increase in the emission intensity. As a result, the accuracy of fluorescence detection increases with the concentration of the target pathogen. In conclusion, fluorescence and MR modalities go hand-in-hand and produce a robust diagnostic tool capable of quantifying a wide range of bacterial contaminations.

To test our hypothesis, *E. coli* O157:H7 cultured in nutrient broth was serially diluted in PBS (1×, pH 7.4) with increasing CFU counts and experimental readings were obtained via both magnetic relaxation and fluorescence emission. Each solution (300 μL) was incubated for 30 min with MFnS (100 μL, [Fe] = 2 mmol) at 37 °C, after which the samples were allowed to cool to room temperature (25 °C) and then transferred into the relaxometer for the collection of $\Delta T2$ values. These results are shown in Figure 1A. As predicted, lower concentrations of bacteria produced dose-dependent changes in $\Delta T2$ values that were more sensitive than at higher CFU counts. An additional assay was conducted to determine the effect of MFnS concentration and is presented in the Supporting Information (Figure S1).

To address these detection limitations at higher bacterial concentrations, fluorescence data were collected from the same samples. The bacterial solutions were removed from the relaxometer and then centrifuged at 2880 g for 10 min to remove any unbound nanosensors. The remaining bacterial cell pellet was then resuspended in 100 μL of PBS (1×, pH 7.4). Each of these samples (80 μL) was added to a 96-well plate, and fluorescence intensities from the samples were read, as shown in Figure 1B. As expected, the fluorescence intensity increased with the corresponding CFU concentrations. The
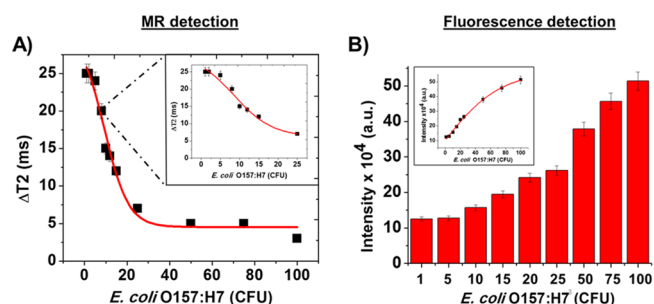

Figure 1. (A) Using our dual-modal MFnS, magnetic relaxation data ($\Delta T2$) were first collected from serial dilutions of *E. coli* O157:H7 in PBS solvent (1×, pH 7.4) (1−100 CFU). It was noted that MR detection of bacteria was highly sensitive at low CFU counts (inset: ranging from 1 to 20 CFU). However, the MR experiments became less sensitive with higher bacterial concentrations (>20 CFU), indicating that MR is more valuable for the detection of early stage bacterial contamination. This is complemented by the additional optical modality of our nanosensor. (B) Fluorescence emission data from the same contaminated samples (inset: linearity plot). Our results showed that the fluorescence detection method is more sensitive at higher CFU counts, whereas it is lacking in sensitivity for low CFU samples. Together, these assays demonstrate the ability of our dual-modality nanosensors to detect bacterial contamination in both early and late stages of development.

amount of emission is significantly higher at greater CFU counts, implying that detection via fluorescence is more effective for later stage bacterial contamination. It is important to note that the intensity does not begin to significantly increase until roughly 20 CFU, which is around the same range at which the magnetic relaxation $T2$ values become saturated. This demonstrates the complementation of the dual modalities of our nanosensor. As our results have shown, the fluorescence detection facet pairs uniquely with the magnetic relaxation capabilities of our nanosensors, which are more sensitive for lower CFUs. Therefore, both early- and late-stage bacterial contaminations can be detected by our multifunctional MFnS, which combine magnetic relaxation and fluorescence in a novel fashion.

To further validate the effectiveness of our MFnS, they were tested in more complex media, including lake water and milk solutions. These media were selected as they are suitable for bacterial growth. Additionally, lake water is often a source of bacterial contamination and milk is a common consumable. These solutions were first prepared by adding MFnS (100 μL, [Fe] = 2 mmol) to serially diluted samples of *E. coli* O157:H7 (300 μL, 1−100 CFU), each containing 200 μL of either lake water or whole milk. These solutions were allowed to incubate for 30 min at 37 °C, and $\Delta T2$ measurements were recorded immediately after the solutions returned to room temperature (25 °C). These MR results (Figure 2A,B for lake water and milk, respectively) produced trends very similar to those obtained in the simple media experiments, shown previously in Figure 1A. The clustering of MFnS around bacteria in a low CFU environment once again resulted in very sensitive detection, but leveled off in the higher CFU range. To address this, the solutions were then centrifuged and the pellets were resuspended for collection of fluorescence data, shown in Figure 2C,D for lake and milk solutions, respectively. The fluorescence readings were also similar to the previous bacterial media tests, as they showed increased sensitivity for higher CFU counts. Together, these assays demonstrated the validity
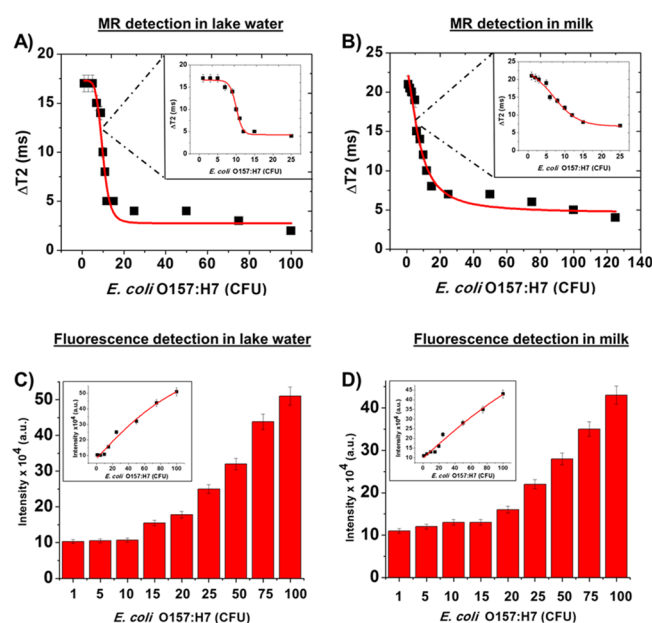
Figure 2. Magnetic relaxation $\Delta T2$ data were collected in more complex media, including (A) lake water and (B) whole milk. Similar to the previous assays, it was noted that detection of bacterial contaminants was more sensitive in the range of 1−20 CFU (insets). Corresponding fluorescence data were collected for both the (C) lake water and (D) milk samples (insets: linearity plots) and showed higher sensitivity with higher CFU counts. Once again, these assays demonstrate the dual detection capabilities of our nanosensors and validate their accuracy in complex media.

of our MFnS in various media, showing that detection is not restricted to only simplified PBS solutions but functions in complex media as well.

Following the detection of *E. coli* O157:H7 in lake water samples, a question was posed regarding whether or not the presence of other bacterial contaminants in the solution would affect the resulting MR and fluorescence data. To further explore this possibility, we designed a number of assays that would allow us to determine the specificity maintained by our MFnS. Toward this end, our nanosensors were tested in nutrient broth solutions with our target, *E. coli* O157:H7, as well as generic *E. coli*, *S. typhimurium*, and a mixture of these. Samples were prepared by incubating 100 μL of our MFnS nanosensor ([Fe] = 2 mmol) with the various targets (300 μL, 10 CFU) for 30 min at 37 °C. Because the only goal of this assay was to determine the specificity of the binding interactions, MR analysis was chosen as the sole method of detection. As can be seen in Figure 3A, little interaction was observed between our nanosensors and the biotargets other than *E. coli* O157:H7. This is due to the specificity associated with our IgG1 antibody-conjugated nanosensors. To further evaluate the specificity of this antibody, we designed another assay to determine if our nanosensors were able to distinguish between viable and nonviable (heat-inactivated) *E. coli* O157:H7 cells. Briefly, 200 μL of nanosensor ([Fe] = 2 mmol) was incubated for 30 min at 37 °C with solutions of contaminated nutrient broth (300 μL, 10 CFU), one with live *E. coli* O157:H7 and the other with heat-killed *E. coli* O157:H7. As shown in Figure 3B, there is little reaction between the MFnS and the heat-inactivated bacteria when compared to the MR data collected from viable *E. coli* O157:H7. These data indicate that our nanosensors specifically target living pathogens. Finally, the MFnS specificity was further demonstrated by analyzing binding between the target bacteria and MFnS which had been conjugated with an isotypic anti-*E. coli* O111 antibody. As was expected, there was little to no reaction between these isotypic MFnS and the target bacteria (Figure 3C). Together, these specificity assays revealed that our nanosensors will produce strong positive signals only in the presence of the desired target bacteria. It is also important to note that our MFnS were able to differentiate between two
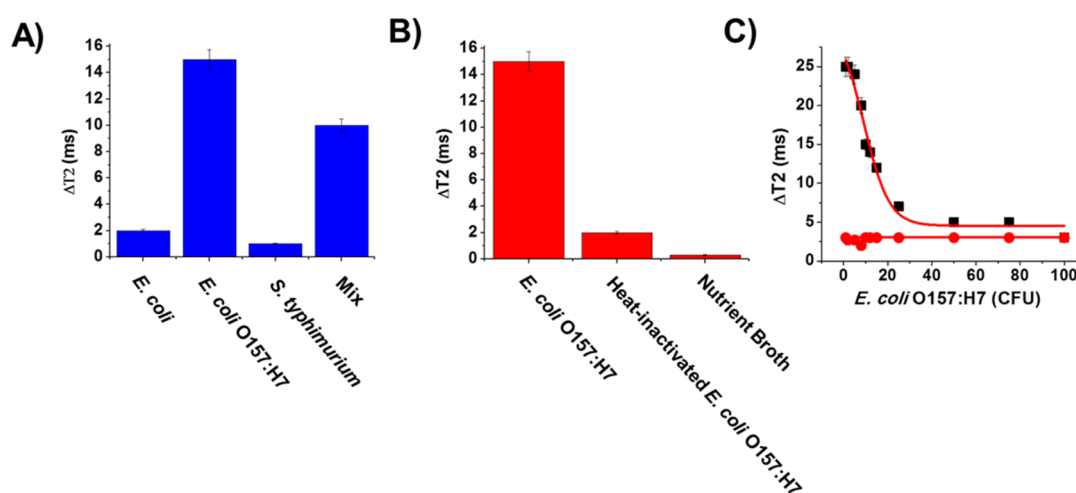
Specificity Assays

Figure 3. Specificity of our nanosensor was tested using MR analysis in nutrient broth solutions of (A) various bacteria cross-contaminants and a mixture. The specificity was further analyzed by (B) heat-inactivating our target bacteria, *E. coli* O157:H7, and collecting MR data. It was clearly shown that our nanosensors have little to no reactivity with nontargeted bacteria and are still able to detect the targeted bacteria in the presence of other contaminants. (C) Additional specificity testing was conducted using an isotypic antibody (red circles, anti-*E. coli* O111), which resulted in little to no binding compared to the O157:H7 antibody-conjugated MFnS (black squares). These assays demonstrated that the nanosensors react only with viable target bacteria, further verifying their validity as a detection tool.

different strains of *E. coli*, as well as living and nonliving. Furthermore, our nanosensors were able to detect the targeted bacteria while in the presence of other nontargeted contaminants, once again displaying the detection capabilities of our MFnS in complex media.

In conclusion, we have designed and synthesized multimodal nanosensors that provide the ability to screen for target pathogens via a double-edged mechanism. These paired detection techniques, magnetic relaxation and fluorescence emission, complement one another and provide a means by which bacterial contamination can be rapidly quantified in both early and late stages of development. Magnetic relaxation and fluorescence alone are limited to specific ranges in which detection results are reliable. MR $\Delta T2$ data are more specific during the early stages of bacterial contamination in which CFU counts are low. In a more developed contamination where the CFU count is much higher, fluorescence emission provides a more accurate detection reading. However, in our case, the pairing of these modalities overcomes these limitations and extends the CFU range in which detection is reliable. In addition to the ability to characterize the development of a bacterial contamination, we have analyzed the specificity of our nanosensors by demonstrating their lack of binding with nontargeted bacteria, as well as heat-inactivated *E. coli* O157:H7. This newly developed multimodal nanosensor technology offers a novel approach to the detection of bacterial contamination, introducing a method for the prevention of water- and foodborne illnesses. Furthermore, these experiments have demonstrated that our nanosensors are efficient with regard to time and are able to detect bacterial contamination in less than an hour. This is much quicker than current gold-standard techniques, including real-time PCR, which can take up to 24 h for data collection.[2] In addition to merits regarding sensitivity and time efficiency, detection via our proposed platform is made more realistic by the growing presence of portable and relatively inexpensive benchtop relaxometers and fluorescence emission readers. Finally, this nanoplatform may be customized for the detection of a wide range of pathogens and applied for the solving of old problems in new ways.

METHODS

Materials. Ferric chloride ($FeCl_3 \cdot 6H_2O$), ferrous chloride ($FeCl_2 \cdot 4H_2O$), hydrochloric acid, and ammonium hydroxide were obtained from Fischer Scientific, ACS reagent grade. Polyacrylic acid (PAA), 2-morpholinoethanesulfonic acid (MES), 1-ethyl-3-(3-(dimethylamino)propylcarbodiimide hydrochloride (EDC), and *N*-hydroxysuccinimide (NHS) were purchased from Sigma-Aldrich. Bacterial strains *E. coli* O157:H7, *Staphylococcus aureus*, and generic *E. coli* were obtained from American Type Culture Collection (ATCC), and the IgG1 antibody (anti-*E. coli* O157:H7 antibody ab75244) was purchased from Abcam. The isotypic antibody (anti-*E. coli* O111) was obtained from KPL. Near-infrared DiI dye was purchased from Invitrogen. The nutrient broth used consisted of beef extract (3 parts), peptone (5 parts), and agar (15 parts).

Synthesis. *Synthesis of Antibody IgG1 Conjugated IONPs: Bioconjugation Chemistry.* To functionalize our nanoparticles with IgG1 antibody, four different solutions were prepared: (1) 4 mL of IONP−COOH (5.0 mmol) added to 1 mL of PBS (pH 7.4); (2) 3 mg of NHS in 250 μL of MES buffer (0.1 M, pH 6.8); (3) 5 mg of EDC in 250 μL of MES buffer (0.1 M, pH 6.8); (4) 5 μg of IgG1, the *E. coli* mAb, in 225 μL of PBS.

Solution 3 was prepared and immediately added to solution 1, followed by the addition of solution 2, after brief mixing. This reaction mixture was incubated for an additional 3 min before dropwise addition of solution 4. The reaction was continued for 4 h at room temperature and then continued at 4 °C overnight. The resulting Ab-conjugated IONPs were purified via magnetic column using PBS (pH 7.4, final concentration [Fe] = 3.5 mmol) to remove any unconjugated antibodies and stored at 4 °C (step A, Scheme 1).

Encapsulation of Fluorescence Dye DiI: MFnS Synthesis. Using a solvent diffusion method, fluorescent dye DiI was encapsulated within the PAA coatings of Ab conjugated IONP (step B, Scheme 1). To 4 mL of antibody-conjugated IONP (3.5 mmol) was added dropwise 2.0 μL of DiI dye (2 mmol) in 100 μL of DMSO with continuous mixing at 1100 rpm. The resulting solution was dialyzed for 12 h using a dialysis bag (MWCO 6−8K) against PBS (pH 7.4, final concentration [Fe] = 2.0 mmol) solution. Successful encapsulation of DiI was confirmed using UV−vis spectrophotometric analysis (Supporting Information, Figure S2A,B) followed by storage in dark conditions at room temperature.

Characterizations. *Spectrophotometric Analysis.* A high-throughput plate reader (TECAN infinite M200 PRO) was used for fluorescence measurement of IONP−DiI−mAb. The successful encapsulation of DiI dye was confirmed by the fluorescence emission at 595 nm (Supporting Information, Figure S2).

Dynamic Light Scattering (DLS) Experiments. The average size distribution and surface charge (ζ-potential) of our functional MFnS were obtained via a DLS technique using Malvern's Nano-ZS90 zetasizer. The average diameters of IONP−COOH and antibody-conjugating IONP (IONP−Ab) were found to be 60.16 and 77.09 nm, respectively (Supporting Information, Figure S3). The ζ-potentials of IONP−COOH and IONP−Ab were found to be −36.8 and −22.3 mV, respectively (Supporting Information, Figure S4).

Bacterial Culture. All bacterial strains were cultured in the corresponding nutrient broth, and the growth of the bacteria was monitored spectrophotometrically to 0.1 absorbance unit; 0.1 mL of bacterial suspension (0.1 OD was serially diluted to different concentrations in nutrient broth, lake water, and milk. A plate-counting method was used to measure the CFU value of different samples.

Collection of Magnetic Relaxation Data. Samples of various CFU counts were prepared in nutrient broth, lake water, and whole milk, depending upon the desired assay. One hundred microliters of MFnS ([Fe] = 2 mmol) was then added to each sample, and the resulting mix was incubated for 30 min at 37 °C. Samples were then transferred to the relaxometer (Bruker mq20, 0.47T) for data collection at 25 °C.

Fluorescence Measurements. The samples prepared for magnetic relaxation data collection were also used for fluorescence reading. The samples were transferred to Eppendorf tubes and centrifuged at 2880 *g* for 10 min. The resulting bacterial pellets were collected after the disassociation of any unbound nanoparticles. The supernatant was discarded, and the pellet was resuspended in 100 μL of PBS (1×, pH 7.4) and then used for fluorescence reading using a plate reader.

ASSOCIATED CONTENT

ⓢ Supporting Information

The Supporting Information is available free of charge on the ACS Publications website at DOI: 10.1021/acsinfecdis.6b00108.

> Detailed synthesis and characterizations of MFnS including ζ-potential, size measurement, and fluorescence property (PDF)

AUTHOR INFORMATION

Corresponding Authors

*(S. Santra) E-mail: ssantra@pittstate.edu. Phone: (620) 235-4861. Fax: (620) 235-4003.
*(T. Banerjee) E-mail: tbanerjee@pittstate.edu. Phone: (620) 235-4749.

Author Contributions

∥S. Sulthana and T. Shelby contributed equally.

Notes

The authors declare no competing financial interest.

ACKNOWLEDGMENTS

REFERENCES

(1) Pandey, P. K., Kass, P. H., Soupir, M. L., Biswas, S., and Singh, V. P. (2014) Contamination of water resources by pathogenic bacteria. *AMB Express* 4, 51.

(2) Law, J. W., Ab Mutalib, N. S., Chan, K. G., and Lee, L. H. (2014) Rapid methods for the detection of foodborne bacterial pathogens: principles, applications, advantages and limitations. *Front. Microbiol.* 5, 770.

(3) Heithoff, D. M., Shimp, W. R., House, J. K., Xie, Y., Weimer, B. C., Sinsheimer, R. L., and Mahan, M. J. (2012) Intraspecies variation in the emergence of hyperinfectious bacterial strains in nature. *PLoS Pathog.* 8, e1002647.

(4) Zhao, X., Lin, C. W., Wang, J., and Oh, D. H. (2014) Advances in rapid detection methods for foodborne pathogens. *J. Microbiol. Biotechnol.* 24, 297−312.

(5) Ishii, S., and Sadowsky, M. J. (2008) *Escherichia coli* in the environment: implications for water quality and human health. *Microbes Environ.* 23, 101−108.

(6) Wang, J., Morton, M. J., Elliott, C. T., Karoonuthaisiri, N., Segatori, L., and Biswal, S. L. (2014) Rapid detection of pathogenic bacteria and screening of phage-derived peptides using microcantilevers. *Anal. Chem.* 86, 1671−1678.

(7) Chiou, C. S., Hsu, S. Y., Chiu, S. I., Wang, T. K., and Chao, C. S. (2000) *Vibrio parahaemolyticus* serovar O3:K6 as cause of unusually high incidence of food-borne disease outbreaks in Taiwan from 1996 to 1999. *J. Clin. Microbiol.* 38, 4621−4625.

(8) Scallan, E., Hoekstra, R. M., Angulo, F. J., Tauxe, R. V., Widdowson, M. A., Roy, S. L., Jones, J. L., and Griffin, P. M. (2011) Foodborne illness acquired in the United States − major pathogens. *Emerging Infect. Dis.* 17, 7−15.

(9) Edberg, S. C., Rice, E. W., Karlin, R. J., and Allen, M. J. (2000) *Escherichia coli*: the best biological drinking water indicator for public health protection. *J. Appl. Microbiol.* 88, 106S−116S.

(10) Ahmed, W., Gyawali, P., and Toze, S. (2015) Quantitative PCR measurements of *Escherichia coli* including Shiga toxin-producing *E. coli* (STEC) in animal feces and environmental waters. *Environ. Sci. Technol.* 49, 3084−3090.

(11) Zhao, X., Hilliard, L. R., Mechery, S. J., Wang, Y., Bagwe, R. P., Jin, S., and Tan, W. (2004) A rapid bioassay for single bacterial cell quantitation using bioconjugated nanoparticles. *Proc. Natl. Acad. Sci. U. S. A.* 101, 15027−15032.

(12) Singh, A., Poshtiban, S., and Evoy, S. (2013) Recent advances in bacteriophage based biosensors for food-borne pathogen detection. *Sensors* 13, 1763−1786.

(13) Chen, J., Tang, J., Liu, J., Cai, Z., and Bai, X. (2012) Development and evaluation of a multiplex PCR for simultaneous detection of five foodborne pathogens. *J. Appl. Microbiol.* 112, 823−830.

(14) LeBlanc, J. J., Li, Y., Bastien, N., Forward, K. R., Davidson, R. J., and Hatchette, T. F. (2009) Switching gears for an influenza pandemic: validation of a duplex reverse transcriptase PCR assay for simultaneous detection and confirmatory identification of pandemic (H1N1) 2009 influenza virus. *J. Clin. Microbiol.* 47, 3805−3813.

(15) Mahony, J. B., Chong, S., Luinstra, K., Petrich, A., and Smieja, M. (2010) Development of a novel bead-based multiplex PCR assay for combined subtyping and oseltamivir resistance genotyping (H275Y) of seasonal and pandemic H1N1 influenza A viruses. *J. Clin. Virol.* 49, 277−282.

(16) Huang, C.-J., Dostalek, J., Sessitsch, A., and Knoll, W. (2011) Long-range surface plasmon-enhanced fluorescence spectroscopy biosensor for ultrasensitive detection of *E. coli* O157:H7. *Anal. Chem.* 83, 674−677.

(17) Alvarez, M. M., Lopez-Pacheco, F., Aguilar-Yanez, J. M., Portillo-Lara, R., Mendoza-Ochoa, G. I., Garcia-Echauri, S., Freiden, P., Schultz-Cherry, S., Zertuche-Guerra, M. I., Bulnes-Abundis, D., Salgado-Gallegos, J., Elizondo-Montemayor, L., and Hernandez-Torre, M. (2010) Specific recognition of influenza A/H1N1/2009 antibodies in human serum: a simple virus-free ELISA method. *PLoS One* 5, e10176.

(18) Han, F., Wang, F., and Ge, B. (2011) Detecting potentially virulent *Vibrio vulnificus* strains in raw oysters by quantitative loop-mediated isothermal amplification. *Appl. Environ. Microbiol.* 77, 2589−2595.

(19) Jayamohan, H., Gale, B. K., Minson, B., Lambert, C. J., Gordon, N., and Sant, H. J. (2015) Highly sensitive bacteria quantification using immunomagnetic separation and electrochemical detection of guanine-labeled secondary beads. *Sensors* 15, 12034−12052.

(20) Farnleitner, A. H., Hocke, L., Beiwl, C., Kavka, G. C., Zechmeister, T., Kirschner, A. K., and Mach, R. L. (2001) Rapid enzymatic detection of *Escherichia coli* contamination in polluted river water. *Lett. Appl. Microbiol.* 33, 246−250.

(21) Wang, Y., Ye, Z., Si, C., and Ying, Y. (2011) Subtractive inhibition assay for the detection of *E. coli* O157:H7 using surface plasmon resonance. *Sensors* 11, 2728−2739.

(22) Meeker, D. G., Jenkins, S. V., Miller, E. K., Beenken, K. E., Loughran, A. J., Powless, A., Muldoon, T. J., Galanzha, E. I., Zharov, V. P., Smeltzer, M. S., and Chen, J. (2016) Synergistic photothermal and antibiotic killing of biofilm-associated *Staphylococcus aureus* using targeted antibiotic-loaded gold nanoconstructs. *ACS Infect. Dis.* 2, 241−250.

(23) Huh, Y. S., Lowe, A. J., Strickland, A. D., Batt, C. A., and Erickson, D. (2009) Surface-enhanced Raman scattering based ligase detection reaction. *J. Am. Chem. Soc.* 131, 2208−2213.

(24) Bui, M-P. N., Ahmed, S., and Abbas, A. (2015) Single-digit pathogen and attomolar detection with the naked eye using liposome-amplified plasmonic immunoassay. *Nano Lett.* 15, 6239−6246.

(25) Kaittanis, C., Naser, S. A., and Perez, J. M. (2007) One-step, nanoparticle-mediated bacterial detection with magnetic relaxation. *Nano Lett.* 7, 380−383.

(26) Chen, Y., Xianyu, Y., Wang, Y., Zhang, X., Cha, R., Sun, J., and Jiang, X. (2015) One-step detection of pathogens and viruses: combining magnetic relaxation switching and magnetic separation. *ACS Nano* 9, 3184−3191.

(27) Santra, S., Kaittanis, C., Grimm, J., and Perez, J. M. (2009) Drug/dye-loaded, multifunctional iron oxide nanoparticles for

combined targeted cancer therapy and dual optical/magnetic resonance imaging. *Small 5*, 1862−1868.

(28) Kaittanis, C., Santra, S., Santiesteban, O. J., Henderson, T. J., and Perez, J. M. (2011) The assembly state between magnetic nanosensors and their targets orchestrates their magnetic relaxation response. *J. Am. Chem. Soc. 133*, 3668−3676.